NITRATE MEDIATED AND HALOGEN ASSISTED ALCOHOL

OXIDATION IN ELECTROCHEMICAL SYSTEMS

Matthew Whalen

December 8, 2020

This thesis has been read and approved by Professor Bart Bartlett, Ph. D.

Signed: _____   Date: 12/05/2020

Faculty Advisor E-mail: bartmb@umich.edu   Phone: (734) 615-9279

Table of Contents

Abstract

There is great potential in finding a pathway to convert biomass waste into a product of commercial value. For example, 5-hydroxymethylfurfural (HMF) is a biomass derivative that has useful functional groups, such as an aromatic ring with oxygen functional groups, which make it useful in forming polymer precursors. A means to oxidize HMF into a polymer precursor is through electrochemistry. Benzyl alcohol ($PhCH_2OH$) is used as a model substitute for HMF because both molecules have similar functional groups. The reaction of $PhCH_2OH$ is favorable when occurring in an organic solvent, such as acetonitrile (MeCN), due to the higher solubility of the substrates and disfavoring the formation of water oxidation intermediates. This thesis focuses on elucidating the mechanism related to nitrate-mediated $PhCH_2OH$ oxidation to benzaldehyde (PhCHO) on platinum electrodes. In the presence of a base, 2,6-lutidene, which is required to render nitrate catalytic, the Faradaic efficiency for PhCHO formation is greater than 80%, with the remaining charge going to an undesired reaction with MeCN solvent.[1]

Given the need for the inclusion of a base to render NO_3^- catalytic and undesired MeCN oxidation, the research focus shifted towards studying whether halogens (chloride and bromide) could be used to assist in the oxidation of ethanol (EtOH) or $PhCH_2OH$ in water. Given the high concentration of chloride in sea water, shifting towards aqueous conditions has the benefit of accessing a readily available resource of sea water and removing offsite C-H bonds in solution, which may interfere with the oxidation of an alcohol. However, given the reduced solubility of $PhCH_2OH$ in water and difficulty in oxidizing it, due to the presence of the aromatic ring, EtOH oxidation became the focus.

Introduction

Section 2.1 Value of Biomass Conversion and Use of Benzyl Alcohol as a Model Substrate:

There has been a growth in research interest in the conversion and usage of biomass obtained from agricultural byproducts or biodegradable waste as a means to generate polymer precursors. Though organic waste is often used as fertilizer or in generating power, another avenue is to convert it into commercially viable chemicals.[2] Bagasse is one such agricultural byproduct from farming sugarcane that amounts to 120 metric tons of waste per year, and since lignin, a polymer composed of aromatics that provides structural support to plants, is a common compound within bagasse, breaking it down into cellulose and then to cyclic compounds serves to provide valuable chemical precursors.[2] The pentose and hexose sugars obtained can then be converted to furfural and 5-hydroxymethylfurfural (HMF). For example, pentose sugars can be easily converted to an intermediate enol and then to HMF at a pH ~0, which can be obtained at concentrations greater than 0.25 M hydrochloric acid (HCl).[3] HMF is the compound that this thesis is focused on oxidizing, since chemicals such as 2,5-diformylfuran (DFF) and 2,5-furandicarboxylic acid can be generated through oxidation, and they serve as renewable polymers to replace similar plastics such as polyesters.[2] Currently, many processes for forming DFF from HMF use metals such as Ru,[4] Pd,[5] or Ni[6] at high pressures; therefore, finding a means

Figure 1: Structures of biomass derived substrates: 5-hydroxymethylfurfural, 2,5-diformylfuran, and 2,5-furandicarboxylic acid.
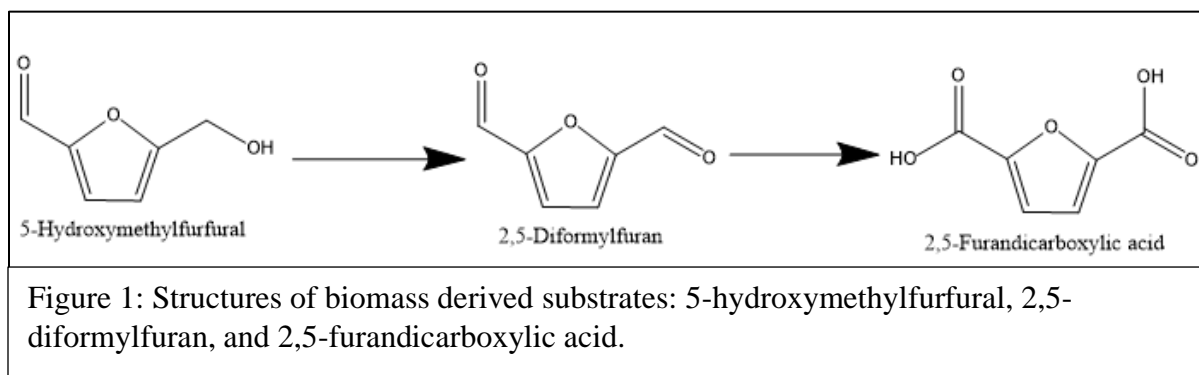
to convert HMF to DFF through electrochemistry without these metals serves to make the process more renewable. This work attempts to use nitrate in place of metal catalysts to drive HMF oxidation to DFF. The electrochemical experiments conducted within this thesis used $PhCH_2OH$ in place of HMF, due to the similarities between the functional groups of HMF and $PhCH_2OH$, such as an aromatic ring and presence of an alcohol group. Therefore, the similarities between the compounds makes for a convenient and cost-effective method to test for the potential conversion of HMF through oxidation.

Section 2.2 Principles of Electrochemistry:

The use of electrochemical techniques applies well when measuring reduction and oxidation processes, since one is able to relate current with the rate of the reaction. Current is defined as the charge (coulombs) passed per second, and through the use of Faraday's constant of 96,485 coulombs per mole of electrons, the current passed can be directly related to the number of moles of reactant converted into a product, when the number of electrons for the process is known. Through the use of electrochemical techniques, such as voltammetry, one can vary the potential over a given range to drive a reduction or oxidation reaction. This occurs due to the movement of the electrode's Fermi level relative to the reaction's redox potential. The movement of the electrode's Fermi level to a more positive potential, relative to the reaction's redox potential, will result in oxidation, since electrons from the species in the solution will flow into the electrode. Conversely, raising the electrode's Fermi level by shifting the potential more negatively will result in the reduction of a species in solution as electrons flow from the electrode into solution. Shifting the electrode's Fermi level serves as a means by which electrons in a state of greater potential energy can move to a region of lower potential energy, and the favorability of

the electron movement can be described through the work associated with moving from one energy level to another.

This is where having a complete circuit is important; otherwise, electrons will not be able to flow through the system. By connecting the electrodes to a device, such as a potentiostat, and having them within a solution that is properly conductive, one can complete a circuit in which oxidation occurs at the anode and reduction occurs at the cathode. Having ions dissolved within the solution allows for them to act as charge carriers across the solution. Solutions with low conductivity result from an increase in solution resistivity from the fewer available pathways for electrons to diffuse, migrate, or convect across the solution to complete the circuit.

Within electrochemistry, popular techniques for understanding redox chemistry include cyclic voltammetry (CV), constant potential coulometry (CPC), and rotating ring-disk electrode (RRDE) experiments. CV experiments are conducted by scanning the working electrode linearly over time from an initial potential to a potential limit, and then reversing the scan.[7] Additionally, a linear sweep voltammetry (LSV) experiment is conducted in the same manner as CV, but without the reverse scan. At each potential step in both an LSV and CV, the current at the working electrode, which pertains to the redox reaction, is plotted against the potential at which it is read. This provides a plot in which one views the current generated as a result of moving the electrode's Fermi level relative to the species in solution. The initial current within a scanned region of an LSV and CV pertains to the kinetics of a reaction, followed by a convoluted region of diffusion and kinetics, and ending with a diffusion-based region. For a CV, this results in a duck shaped trace. However, should the reaction not be diffusion limited, then one will observe an exponential trace for the redox reaction in an LSV or CV experiment. Lastly, varying the scan rate in LSV and CV experiments allows for the identification of different processes within a

reaction; however, as the scan rate is increased, the current will be increased, and this will result in greater current-resistance distortion and the masking of redox processes within a trace.

CPC allows for studying the reactivity of a species in solution, while all other species in solution remain inactive, by picking a potential at which only the target species is active.[8] Therefore, the current measured over time at a fixed potential pertains to the target species in solution. This is particularly useful for measuring the amount of charge passed through the experiment, which can be converted to the number of moles reacted with the use of Faraday's constant. Additionally, one can measure the amount of a target product produced, and if the number of electrons needed for the reaction is known, then one can calculate how much charge went towards the formation of the target product at a given potential, which refers to the Faradaic efficiency of the system.

RRDE experiments allow for solving the kinetics of a redox reaction through controlling the velocity of the solution, which makes the steady-state mass transport rate known.[9] As a result, the current pertaining to the mass transport is known, and the remaining current measured in the experiment pertains to the current contribution by the reaction's kinetics. Additionally, plotting one over the mass transport current versus the square root of the rotation rate allows one to solve for the diffusion coefficient of a species.[9] Another use of RRDE is to hold the disk at a constant potential to reduce or oxidize a species, and then the new species can be reversed to the original at the ring, which conducts an LSV. This allows for identifying redox states of a reaction and if a species is involved in another reaction, which would be indicated by less current measured at the ring for the regeneration of the initial species than there would be expected if no side reaction occurred.

Section 2.3 Precedence for Nitrate as a Mediator:

The oxidation of a nitrate anion (NO_3^-) to a nitrate radical ($NO_3\bullet$), within the solution, is a one-electron process that generates a highly reactive product, which can go on to oxidize a substrate, thereby providing an oxidized substrate at a lower potential than normally possible. The oxidation of an alcohol by $NO_3\bullet$ has been proposed to occur through hydrogen atom transfer (HAT).[10] Recent studies have looked at the use of nitrate anions to indirectly oxidize alcohols within photocatalytic systems. In the presence of cadmium sulfide nanowires, it was proposed that the photochemical generation of a $NO_3\bullet$ leads to the oxidation of $PhCH_2OH$ to $PhCHO$ within MeCN.[11] On bismuth(III) vanadate in MeCN, the indirect photoelectrochemical oxidation of $PhCH_2OH$ to $PhCHO$ had a reduced potential in the presence of nitrate anions, and it was proposed that $NO_3\bullet$ formed HNO_3 through hydrogen atom transfer with $PhCH_2OH$.[12] These recent results inspired further research regarding the mechanism and behavior of NO_3^-/ $NO_3\bullet$ mediation on platinum within MeCN, which is further discussed within the results of the thesis in chapter 4.

Section 2.4 Precedence for Chloride and Bromide in Assisting Alcohol Oxidation:

Previous studies have found that primary and secondary alcohols could be selectively oxidized with the addition of hypochlorite and 2,2,6,6-tetramethylpiperidine-1-oxyl (TEMPO), which acts as a catalyst.[13,14] In this system, hypochlorous acid served as an oxidizing agent to regenerate TEMPO, after it is reduced from reacting with an alcohol, and produce water and hydrochloric acid.[13,14] Given the natural abundance of chloride in sea water, accessing chloride oxidation of alcohols serves as a renewable means to achieve oxidized alcohols in the form of aldehydes and carboxylic acids. Oxidizing chloride into chloride radical creates a strong oxidizing agent that may react with an alcohol substrate or water. Should chloride radical react

with water, hypochlorous acid may form, which could also serve to oxidize the alcohol. This mechanism may be similar for bromide oxidation, which would form hypobromous acid that could go on to oxidize an alcohol, especially in the case where TEMPO serves as a catalyst.[15] Therefore, understanding the mechanism and selectivity of these systems in oxidizing alcohols may provide a novel means of obtaining a cleaner means to form oxidized alcohol products. Within the framework of these chloride and bromide systems, the oxidation of $PhCH_2OH$ to PhCHO, as a model for HMF to DFF conversion, was attempted, and the oxidation of ethanol was also tried. Acetaldehyde and acetic acid are produced upon oxidizing ethanol, and they are also important commercial chemicals that are therefore worth attempting to selectively produce. Compared to $PhCH_2OH$, ethanol is a smaller, simpler, and more soluble molecule in water, and these characteristics of ethanol may result in obtaining higher selectivity for oxidizing ethanol within the chloride and bromide systems.

Materials, Methods, and Analysis

This chapter has been adapted from the manuscript *Base-Assisted Nitrate Mediation as the Mechanism of Electrochemical Benzyl Alcohol Oxidation.*[1]

Section 3.1 Materials:

Lithium nitrate ($LiNO_3$), lithium hexafluorophosphate ($LiPF_6$), benzyl alcohol$-\alpha,\alpha-d_2$, and nitric acid (HNO_3) were purchased from Sigma Aldrich; hydrochloric acid (HCl) and acetonitrile (MeCN) were purchased from Fisher Scientific; benzyl alcohol ($PhCH_2OH$), chlorobenzene, and 2,6-lutidine were purchased from Acros Organics. All were used without further purification. Tetrabutylammonium hexafluorophosphate (Bu_4NPF_6) was purchased from TCI and purified through hot ethanol recrystallization. To achieve 50 mM $LiNO_3$, mixtures of $LiNO_3$, MeCN and $PhCH_2OH$ were prepared and then sonicated under heat (~50°C) for 20 minutes to give a clear, colorless solution.

Additionally, sodium chloride (NaCl) was purchased from Fisher Scientific, sodium sulfate (Na_2SO_4) was purchased from Sigma Aldrich, sodium bromide (NaBr) was purchased from J. J. Baker, 2,2,6,6-tetramethylpiperidine-1-oxyl (TEMPO) was purchased from Sigma Aldrich, and 200 proof ethanol was purchased from Decon Laboratories. Aqueous solutions were composed of Millipore water and adjusted to pH 3 for chloride solutions and pH 5.4 for bromide solutions.

Section 3.2 Experimental Setup and Methods:

Cyclic and linear sweep voltammetry was conducted using either a CH Instruments Electrochemical Workstation 660C, 760E, or 1000A with a CHI Pt disk electrode (area = 0.0314 cm^2). Working electrodes were polished using a slurry of 0.05-micron alumina powder in deionized water on a MicroCloth pad. For chloride and bromide experiments, a PtO_2 working

electrode was generated from oxidizing CHI Pt for 1 hr in a 1 M HCl aqueous solution, while stirring. A silver wire was used as the reference electrode and inserted into a sealed glass tube with a Vycor tip and filled with the electrolyte solution. The counter electrode was either a graphite rod or a Pt wire (~0.33 cm^2), of which the latter was cleaned between experiments by dipping into aqua regia for 15 seconds. Unless otherwise stated, voltammetry experiments were conducted at a scan rate of 25 mV/s.

Constant potential coulometry (CPC) and constant current coulometry (CCC) experiments were conducted using a custom built two-compartment glass cell separated by either an ultra-fine glass frit, Nafion membrane, or Sterlitech polypropylene filter paper with a pore size of 0.1 micron. The working compartment contained 12 mL of solution, and the counter compartment had 8 mL of solution for constant potential coulometry experiments. For constant current coulometry, the working compartment contained 15 mL of solution, and the counter compartment contained 10 mL of solution. CPC utilized a Pt wire working electrode (area: ~0.35 cm^2) with a silver wire reference electrode and graphite counter, as used in the voltammetry experiments. Over the course of the CPC experiment, the working compartment solution was agitated using a stir bar. CCC had the same setup as CPC experiments, except a Pt disk electrode was used for CCC.

Rotating ring-disk electrode (RRDE) experiments were conducted at 30 Hz with a Pt ring and disk on a RRDE-3A version 1.2 apparatus from CH Instruments. The ring and disk were polished using a 0.05-micron Alpha Alumina slurry water on a MicroCloth pad. After polishing, the ring and disk were sonicated in deionized water for 10 minutes. The ring and disk were then inserted into the fixture and dipped in aqua regia for 15 seconds, and they were then rinsed with Millipore water. Finally, the RRDE assembly spun at 30 Hz in MeCN for 5 minutes. The now

cleaned RRDE assembly was placed into 35 mL of the analyte solution, and a graphite rod

counter and silver wire reference electrode were then placed into the solution.

Section 3.3 Product Analysis:

Substrate and product concentrations were measured using GC-FID by periodically

removing an aliquot (10 µL) from the reaction mixture and combining with a chlorobenzene

standard (50 µL of a 21.6 mM standard) and MeCN (940 µL). The samples were analyzed on

either a Shimadzu QP-2010 GC/MS or Thermo Fisher Trace 13-10 gas chromatograph equipped

with a capillary column and FID detector. During analysis, the column oven was warmed from

40°C to 290°C at a 10°C/min ramp rate. Quantification was enabled by the integration ratio of

the analyte and chlorobenzene signals in relation to an obtained calibration curve. Additionally,

nuclear magnetic resonance with a 500 MHz instrument was used to quantify and identify

products.

Nitrate Mediated Benzyl Alcohol Oxidation in Acetonitrile

This chapter has been adapted from the manuscript *Base-Assisted Nitrate Mediation as the Mechanism of Electrochemical Benzyl Alcohol Oxidation.*[1]

Section 4.1 Proposed Mechanism:

This section serves to provide an overview of the proposed mechanism of base-assisted nitrate (NO_3^-) mediation of $PhCH_2OH$ oxidation, which will be explored in further detail in subsequent sections. Figure 2 shows the proposed mechanism within a two-compartment cell.
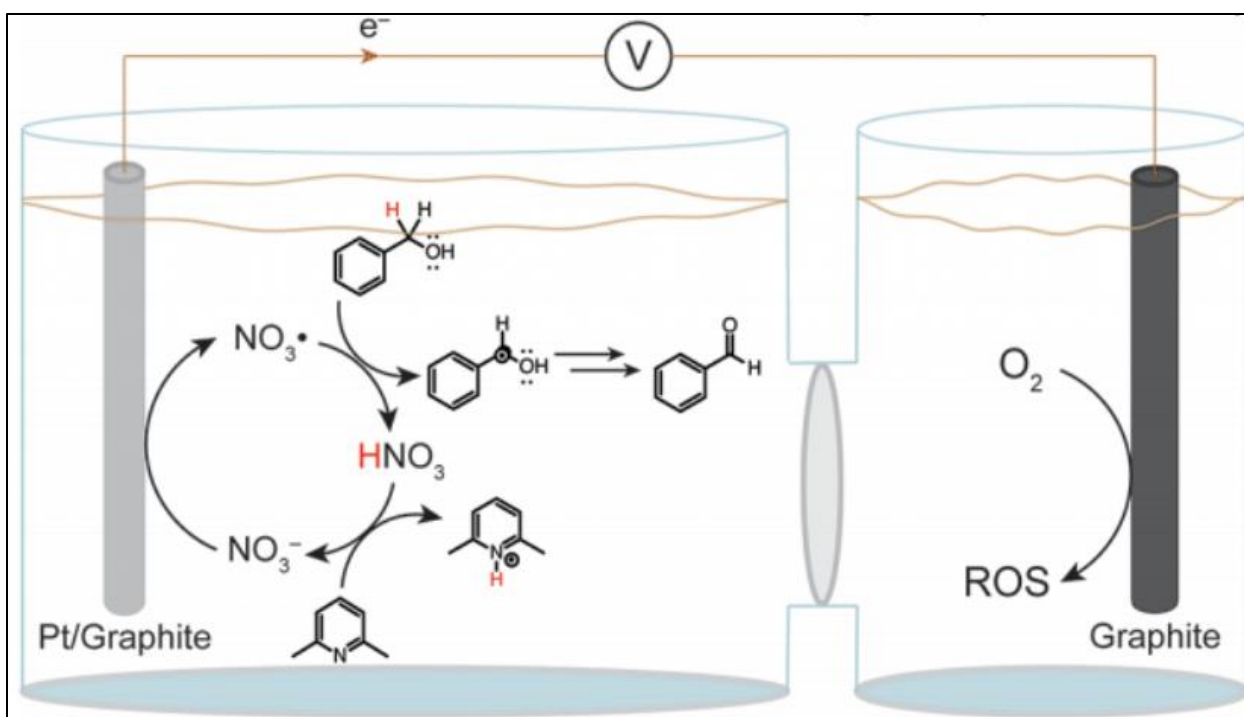

Figure 2: Electrochemical oxidation of nitrate to nitrate radical, which oxidizes $PhCH_2OH$ to generate HNO_3, on Pt within MeCN. 2,6-Lutidine acts as a Brønsted base to regenerate nitrate.

Figure 2 shows NO_3^- diffusing to the anode (Pt/graphite electrode) surface where it is oxidized to $NO_3\bullet$ at a positive potential around 1.5 V versus the ferrocenium/ferrocene couple ($Fc^{+/0}$), as shown in Figure 3a. The $NO_3\bullet$ then reacts through hydrogen atom transfer at the benzylic carbon position to generate nitric acid (HNO_3), which is a weak acid in MeCN, and a benzyl alcohol radical, which decomposes into PhCHO. In the presence of a base, such as 2,6-

10

lutidine, HNO_3 is deprotonated to regenerate NO_3^-, thereby rendering the system catalytic. In the event where a Brønsted base is not present, the oxidation of NO_3^- is diffusion limited. Also, as shown in the counter compartment in Figure 2, oxygen (O_2) is reduced to a reduced oxygen species (ROS) within MeCN, and depending on the conditions, ROS may react with HNO_3 to generate water and nitrate; however, within the two compartment cell, this is not permitted due to the filter membrane that separates the compartments.

Section 4.2 Effect of Nitrate on Benzyl Alcohol Oxidation:

In the absence of a mediator, $PhCH_2OH$ is oxidized at about 1.7 V versus $Fc^{+/0}$ on a platinum electrode, so a potential of 1.68 V versus $Fc^{+/0}$ was chosen for constant potential coulometry (CPC), because this potential correlates with peak NO_3^- oxidation and minimum $PhCH_2OH$ oxidation, as shown in the linear sweep voltammetry (LSV) traces in Figure 3a. Figure 3b shows that when conducting CPC at 1.68 V versus $Fc^{+/0}$, almost no current is generated with $PhCH_2OH$ alone or with lithium hexafluorophosphate ($LiPF_6$), thereby resulting in a Faradaic efficiency of 0%,
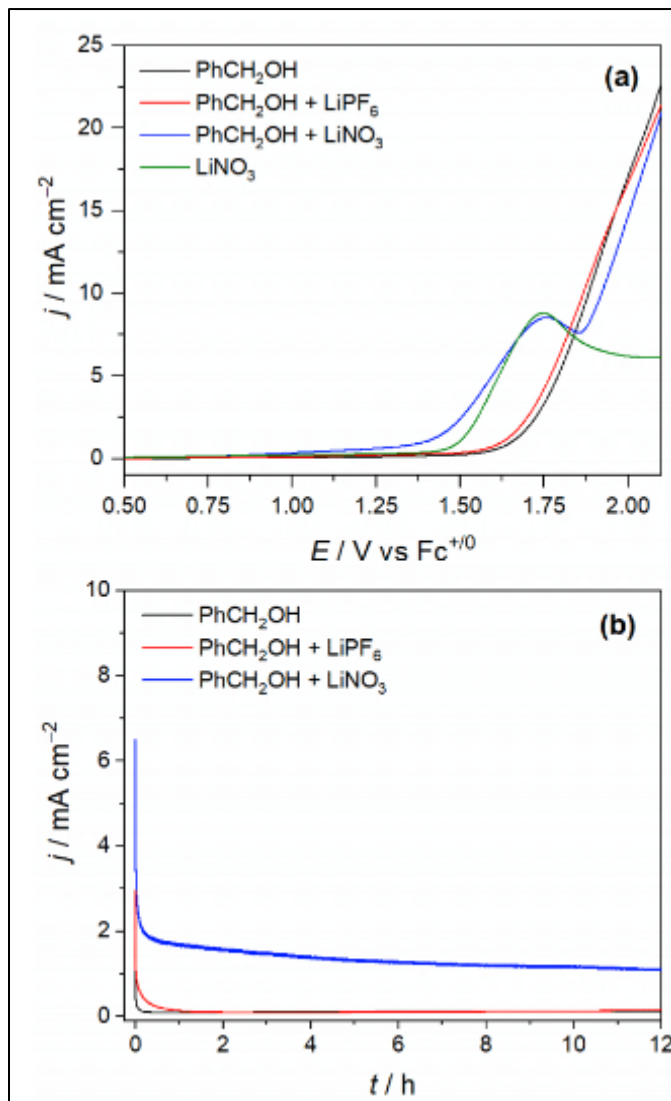

Figure 3: (a) LSV on Pt in MeCN with 100 mM Bu_4NPF_6 under the listed conditions, where $[PhCH_2OH] = 250$ mM and $[LiNO_3] = [LiPF_6] = 50$ mM; (b) CPC performed at 1.68 V vs $Fc^{+/0}$ under the listed conditions using a Pt wire electrode.

which considers the charge passed that went to the formation of PhCHO. However, when $LiNO_3$ is added to the solution, a higher current is observed, and PhCHO product is observed. When comparing the quantity of PhCHO to the charge passed for the 2-electron oxidation, a Faradaic efficiency of $80 \pm 16\%$ is obtained. This indicates that at the same potential being passed for 12 hours, 80% of the charge passed went towards the formation of PhCHO, through the oxidation of NO_3^- to $NO_3\bullet$, which then reacts with $PhCH_2O$. This result indicates that, in the presence of NO_3^-, the oxidation of $PhCH_2OH$ to PhCHO is accessible at 1.68 V versus $Fc^{+/0}$, which would otherwise occur at a higher potential without NO_3^-.

Section 4.3 Nitrate Radical Reactivity:

The oxidation of NO_3^- to $NO_3\bullet$ is irreversible, as demonstrated by the CV trace of lithium nitrate ($LiNO_3$) in Figure 4a. Even when scanning at higher rates, detection of the reduction of the $NO_3\bullet$ back to NO_3^- is not observed. This may indicate that the $NO_3\bullet$ is highly reactive and reacts with the MeCN solvent before it can be reduced and detected through cyclic voltammetry. As a potential means to detect the $NO_3\bullet$, the solvent was

Figure 4: (a) CV on Pt in MeCN with 100 mM $LiPF_6$, 100 mM Bu_4NPF_6 or 50 mM $LiNO_3$ at 25 mV/s. (b) Scan rate dependent CV traces on Pt in MeCN with 100 mM Bu_4NPF_6 and 50 mM $LiNO_3$ at 25, 50, 100, 250, 500, and 1000 mV/s.
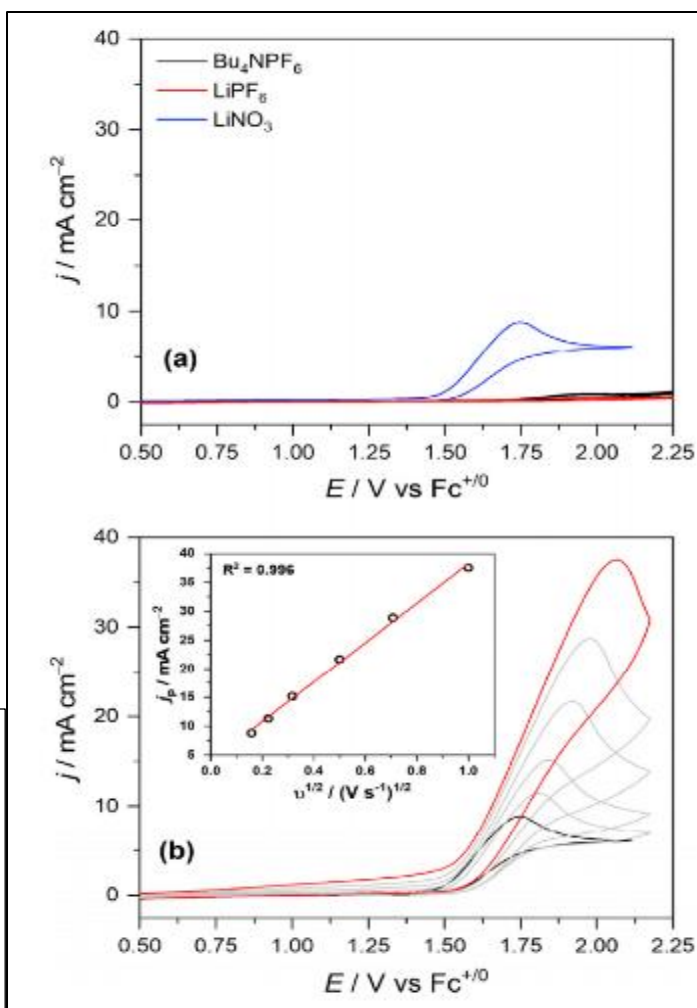
changed from MeCN to one without available C-H bonds that the $NO_3\bullet$ could react with, such as trichloroacetonitrile; however, the supporting electrolyte Bu_4NPF_6 was insoluble in such solvents, and this resulted in low conductivity and the inability to conduct CV scans. Rotating ring disk electrode experiments were then conducted to attempt to further understand the $NO_3\bullet$ reactivity and perceived irreversibility, which is further discussed in Section 4.4. Additionally, based on the linear dependence on the square root of the
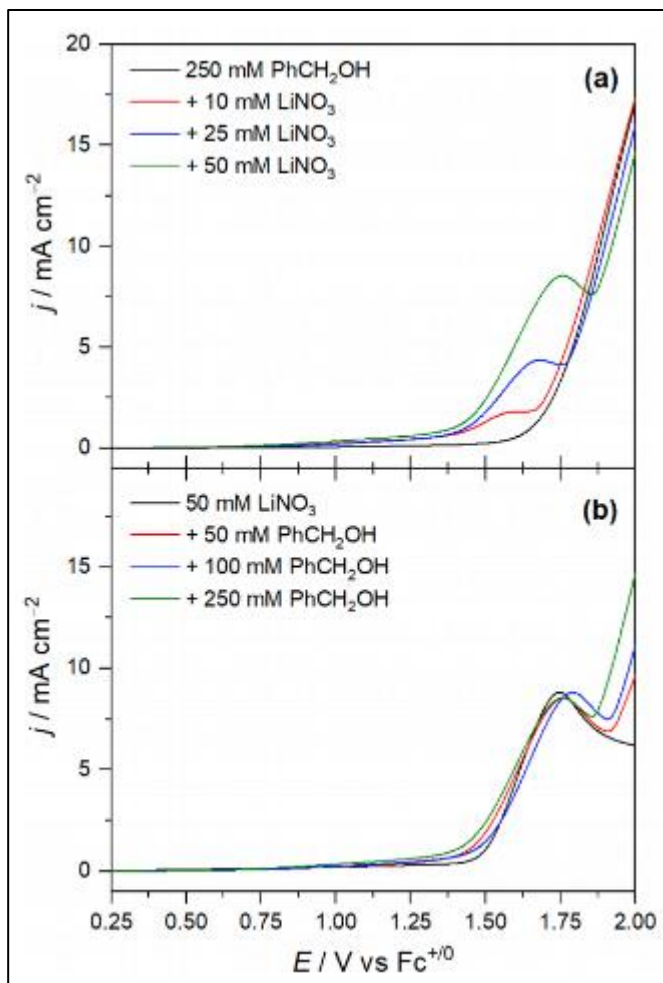

Figure 5: (a) LSV on Pt in MeCN with 100 mM $LiPF_6$, measuring current dependence on [$LiNO_3$] and (b) current dependence on [$PhCH_2OH$].

scan rate, NO_3^- oxidation can be described as diffusion controlled, as shown in Figure 4b. This indicates the rate at which the NO_3^- is oxidized depends on the rate at which NO_3^- can reach the electrode, and as the supply of NO_3^- within the solution diminishes, so will the current associated with NO_3^- oxidation.

To understand the rate dependence of NO_3^- and $PhCH_2OH$ in MeCN, linear sweep voltammograms (LSV) were collected (Figure 5). Figure 5a shows that there is a linear relationship between the concentration of $LiNO_3$ and peak current observed, which indicates that

there is a first order rate dependence on NO_3^-. However, when the concentration of $PhCH_2OH$ was adjusted and $LiNO_3$ concentration was held constant, as shown in Figure 5b, there is no

change in the peak current with or without the presence of $PhCH_2OH$, thereby indicating that $PhCH_2OH$ has a zero-order rate dependence. Figure 5 therefore indicates that NO_3^- oxidation to $NO_3\bullet$ is the rate determining step in the reaction in which $PhCH_2OH$ is oxidized to $PhCHO$.

Given that NO_3^- oxidation is the rate determining step, then $PhCH_2OH$ oxidation is presumed to occur at a faster rate. Therefore, it would be expected that there would be no primary kinetic isotope effect when conducting an LSV scan with deuteration of the α-position on $PhCH_2OH$, as shown in Figure 6. Since the current in the LSV scans of 250mM proteo- or deutero-benzyl alcohol is relatively the same and the two scans overlay nearly exactly, no
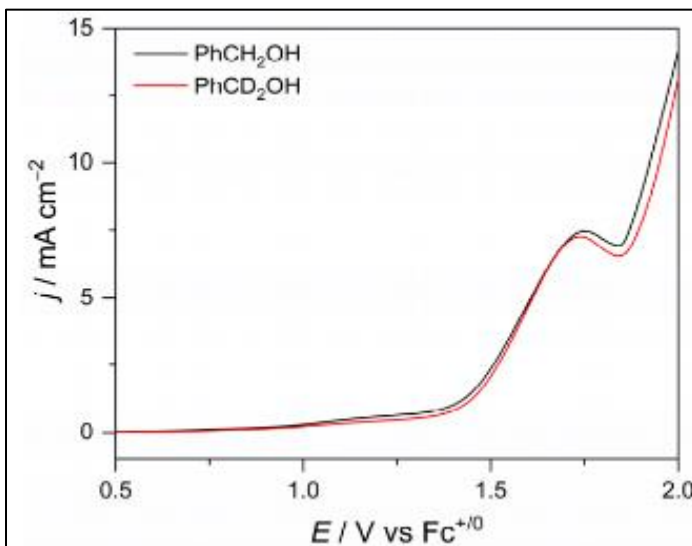

Figure 6: LSV on Pt in MeCN with 50 mM $LiNO_3$, 100 mM Bu_4NPF_6, and 250 mM of proteo- or deutero-PhCH2OH.
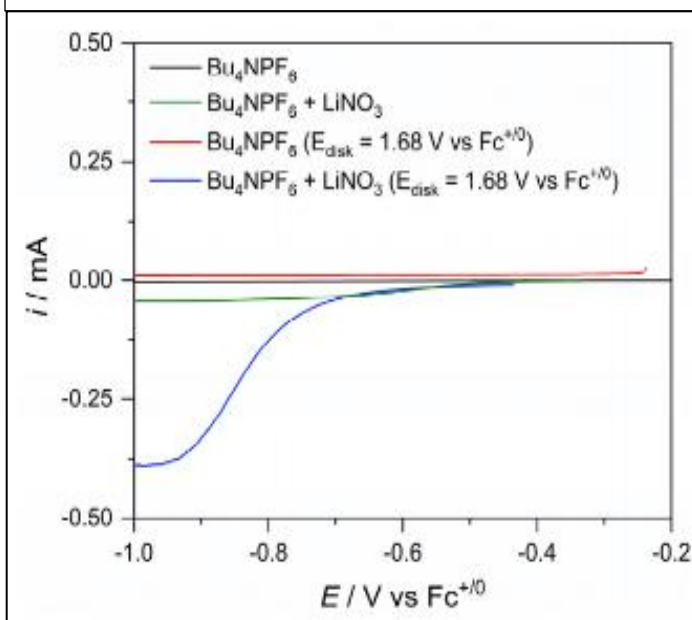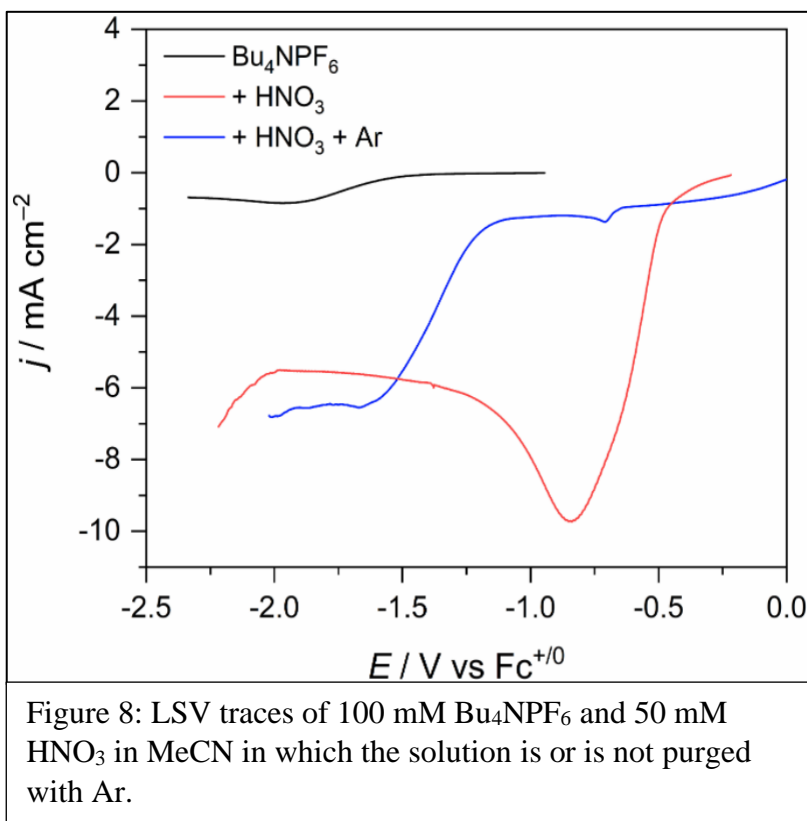

Figure 7: LSV traces of ring current from rotating ring-disk experiments at a rotation rate of 30 Hz with 100 mM Bu_4NPF_6 and 50 mM $LiNO_3$ in MeCN.

primary kinetic isotope effect is observed. This result makes since given PhCH$_2$OH's zero order rate dependence.

Section 4.4 Proton Coupled Oxygen Reduction:

As previously stated, to further understand the NO$_3\bullet$ reactivity, rotating ring disk experiments were conducted to ascertain whether the NO$_3\bullet$ reduction could be observed. In theory, one may think that when NO$_3^-$ is oxidized at a Pt disk held at a constant potential of 1.68 V versus Fc$^{+/0}$, one may then observe the NO$_3\bullet$ reduced at the ring, while it performs an LSV. However, the reduction observed at the ring occurs at a potential (-0.7 V versus Fc$^{+/0}$), which is far too negative from NO$_3^-$ oxidation at 1.5 V versus Fc$^{+/0}$, as shown in Figure 7. Given that oxygen reduction can occur on negatively polarized electrodes, LSV scans were performed with HNO$_3$, and this indicated that the formation of HNO$_3$, upon hydrogen atom transfer, facilitates the reduction of oxygen species, through the acidification of MeCN. Therefore, NO$_3^-$ can be rendered catalytic in the presence of oxygen, which acts as a base upon being reduced. This result is further corroborated when the MeCN solution is purged with argon gas, which is shown in Figure 8 where the peak associated with


Figure 8: LSV traces of 100 mM Bu$_4$NPF$_6$ and 50 mM HNO$_3$ in MeCN in which the solution is or is not purged with Ar.

proton-coupled oxygen reduction at -0.7 V versus Fc$^{+/0}$ disappears after purging.

Section 4.5 Effect of Adding a Base:

2,6-Lutidine was chosen as a base for the LiNO$_3$ and PhCH$_2$OH system due to its lack of involvement in Pt electrocatalysis, and 2,6-lutidinium, the conjugate acid, has a high enough p$K_{a,}$ $_{MeCN}$ of 14.1 to deprotonate HNO$_3$. Figure 9a shows LSV scans with base present and the effect it has on NO$_3^-$ oxidation. As shown by the green and yellow traces in Figure 9a, when 2,6-lutidine is present, NO$_3^-$ loses its diffusion limited profile and takes on a catalytic current profile. This new profile characteristic is attributed to the deprotonation of HNO$_3$ to NO$_3^-$, which allows for the regeneration of NO$_3^-$. When conducting CPC, Figure 9b shows how the addition of 2,6-lutidine leads to an increase in current, while the Faradaic efficiency remained relatively the same at 83%, versus 80% without 2,6-lutidine. Additionally, the various conditions in Figure 9b show

Figure 9: (a) LSV on Pt with 50 mM LiNO$_3$, 250 mM PhCH$_2$OH, and 25 mM 2,6-Lutidine in MeCN. (b) CPC at 1.68 V vs Fc$^{+/0}$ on Pt with 0.5 mM LiNO$_3$, 250 mM PhCH$_2$OH, and with or without 25 mM 2,6-Lutidine.
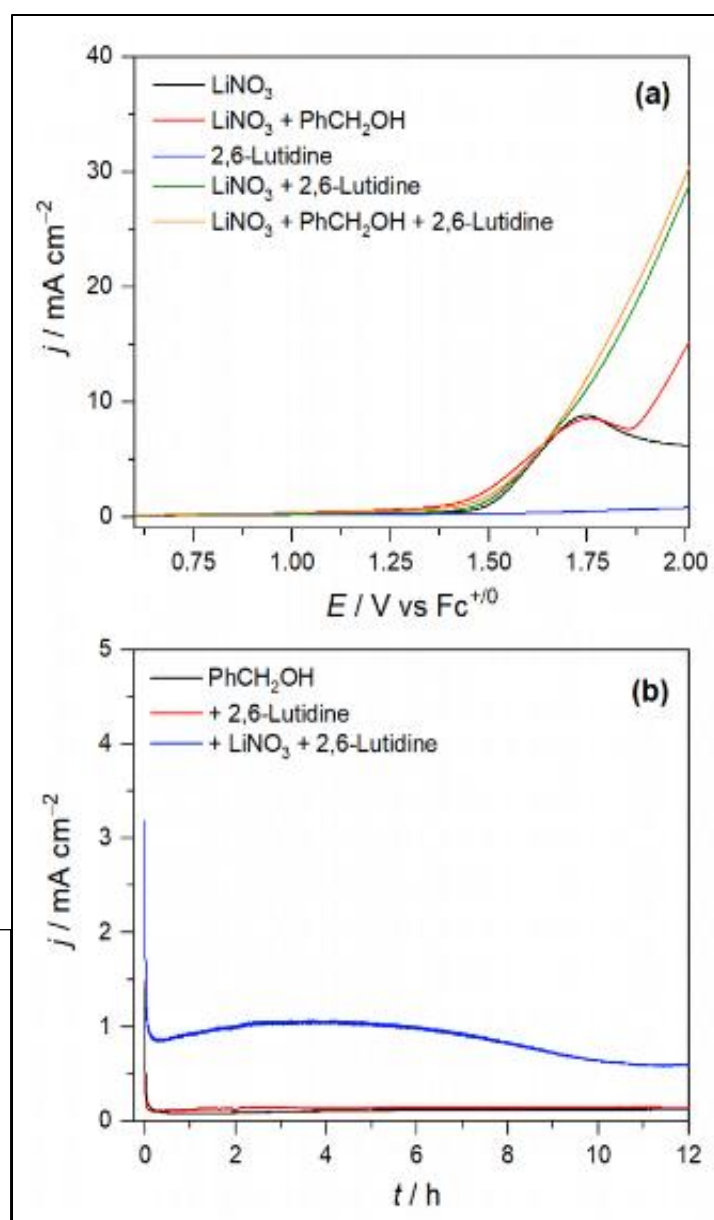
that 2,6-lutidine only improves the current when NO_3^- is present, indicating that 2,6-lutidine alone does not increase the current. The concentration of PhCHO produced is 5 mM in the blue trace of Figure 9b, which is ten times larger than the concentration of NO_3^- in solution (0.5 mM). This result indicates the catalytic nature of NO_3^-, in the presence of base, given that it would require the regeneration of NO_3^- to convert
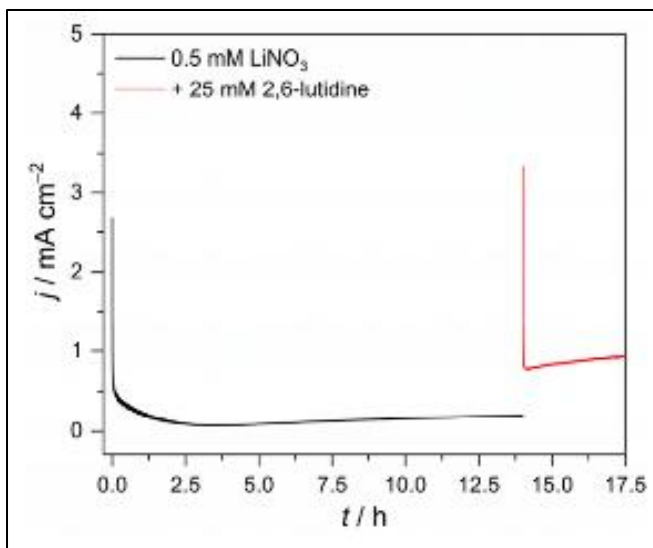

Figure 10: CPC at 1.68 V vs $Fc^{+/0}$ on Pt with 0.5 mM $LiNO_3$ and 250 mM $PhCH_2OH$; the addition of 2,6-lutidine is shown by the red trace at 14 h.

more $PhCH_2OH$ than there is NO_3^- present. Given that the conversion to HNO_3 is irreversible without base, a lower current for NO_3^- oxidation is seen when 2,6-lutidine is not present in CPC experiments, demonstrating the consumption of NO_3^- in solution and the inability to oxidize anymore $PhCH_2OH$ substrate, as shown in Figure 10. When CPC is conducted with 0.5 mM $LiNO_3$, the current drops to nearly zero due to the rapid consumption of NO_3^-; however, when 2,6-lutidine is introduced 14 hours into the experiment, a large current recovery is shown by the red trace in Figure 10. This indicates that NO_3^- has now become catalytic, such that its rapid deprotonation allows NO_3^- to be continuously oxidized and able to react with $PhCH_2OH$.

Of final note, 20% of the faradaic efficiency in CPC experiments does not pertain to $PhCH_2OH$ conversion to PhCHO. This remaining percentage was found to result from the formation of MeCN oligomers. Therefore, the $NO_3 \bullet$ may react with MeCN, and the oxidized MeCN species may go on to react with itself. This demonstrates an unavoidable off target
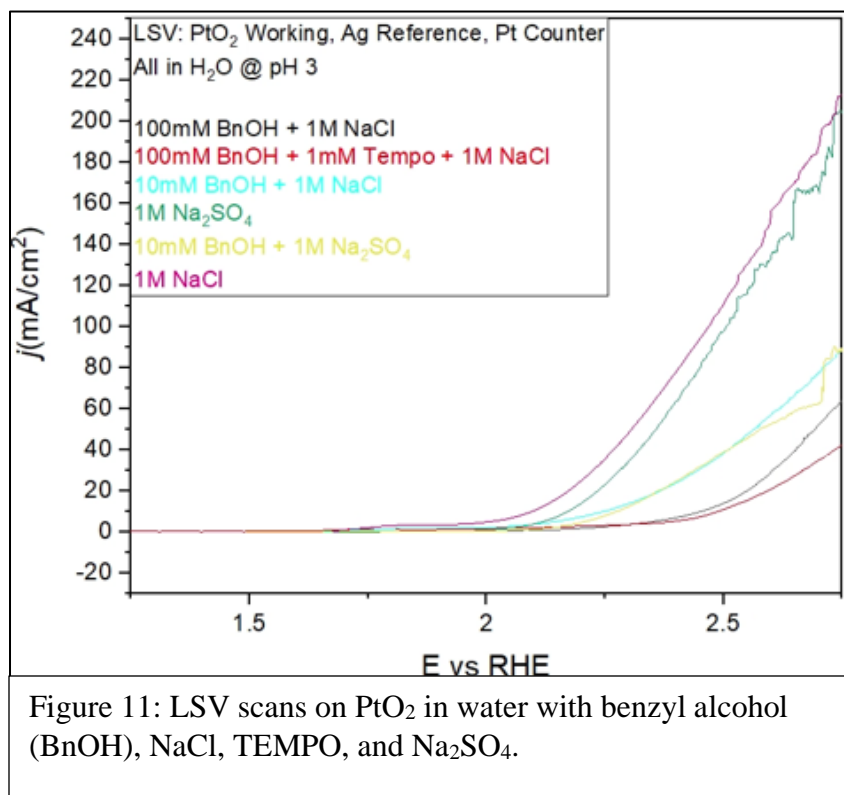
oxidation that occurs with organic solvents, and this limitation is therefore problematic in any

organic solvent in which NO_3^- is used as a mediator for alcohol oxidation.

Bromide and Chloride Assisted Alcohol Oxidation in Water

Section 5.1 Chloride Assisted Benzyl Alcohol Oxidation:

Given the limitations of the NO_3^- system in MeCN, which is the side reaction of NO_3^- with the solvent and the need for a base to render NO_3^- catalytic, the focus shifted towards attempting to understand whether halogens in aqueous conditions could be used to oxidize an alcohol. Chloride (Cl^-) was the initial focus due to its natural abundance in sea water. Therefore, linear sweep voltammograms (LSV) scans were taken of various conditions with TEMPO, $PhCH_2OH$, sodium chloride (NaCl), and sodium sulfate (Na_2SO_4), as shown in Figure 11. PtO_2 was used as the electrode because Pt oxidizes in water with the presence of halogens; therefore, a pretreatment is performed such that Pt oxidation does not convolute the experiments as one attempts to understand halogen assisted alcohol oxidation. Initial LSV results indicated that Cl^- did not improve the current, when compared to sulfate, which is inert within this potential scan range. Additionally, Faradaic efficeincies of 10% or lower were observed in conditions in which a combination of TEMPO, Cl^-, $PhCH_2OH$, and ultraviolet radiation were applied during constant current coloumetry (CCC),

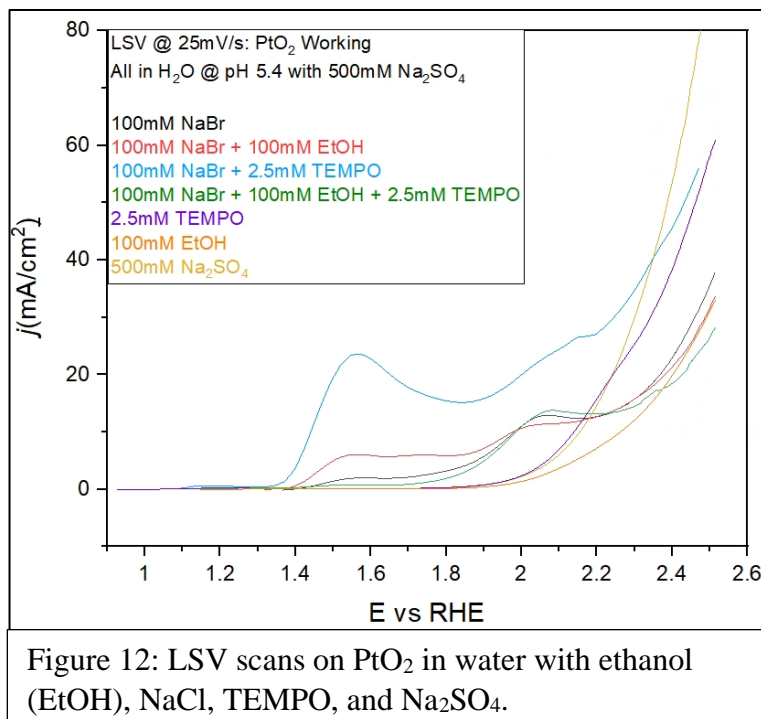Figure 11: LSV scans on PtO_2 in water with benzyl alcohol (BnOH), NaCl, TEMPO, and Na_2SO_4.

which was used to generate a measurable amount of product within a short timeframe of 3 hours. TEMPO was introduced into the system because it can mediate oxidation of alcohols, with a halogen acting to deprotonate and regenerate TEMPO after it oxidizes an alcohol; however, no significant improvements were observed with the addition of TEMPO. Additionally, ultraviolet radiation can excite Cl^- and increase its reactivity; however, no improvement was seen when performing CCC under ultraviolet radition. Given that the majroity of the current passed during CCC does not go towards the formation of an oxidized alcohol product and that there is no improvement in current density with the addition of Cl^- in LSV scans, this project was not further pursued.

Section 5.2 Bromide Assisted Ethanol Oxidation:

Given poor results from Cl^- assisted $PhCH_2OH$ oxidation, the focus shifted towards bromide (Br^-) assisted oxidation of ethanol (EtOH) in water. Br^- has the benefit of being oxidized at a lower potential than Cl^-, and EtOH is more soluble in water than $PhCH_2OH$. Additionally, EtOH oxidation products, such as acetic acid, are valuable commercial products, so attempting to produce such chemicals electrochemically is a worthwhile endeavor.

The LSV traces conducted on PtO_2 in Figure 12 show that the addition of Br^- and TEMPO to the system increase the observed current density, and Br^- oxidation occurs at a lower potential than EtOH; therefore, EtOH oxidation should be accessible at a lower potential. However, when conducting CCC, Br^- alone has a Faradiac efficiency of 18.1% towards the formation of acetaldehyde, acetic acid, and acetal from EtOH, but this can be enhanced with the addition of TEMPO to the system. Additionally, CCC of a Br^- and TEMPO solution provide an

initial Faradaic efficiency of 36.4% towards the formation of acetaldehyde, acetic acid, and acetal from EtOH, but if the solution is allowed to sit, the solution color changes from orange to clear, and a Faradaic effeciency of 59.5% is observed. This result inidcates that an excess of Br⁻ may be oxidized during CCC, and the

Figure 12: LSV scans on PtO$_2$ in water with ethanol (EtOH), NaCl, TEMPO, and Na$_2$SO$_4$.

reaction between TEMPO and EtOH is slow in comparison; therefore, if the solution is allowed to react while sitting, more EtOH is oxidized and the excess oxidized Br⁻ species (OBS) react with TEMPO. Furthermore, it appears that OBS may not directly oxidize EtOH, but rather TEMPO reacts with EtOH, and OBS serve to regenerate TEMPO within the solution. This is supported by the lower Faradiac effeciency for Br⁻ only and a Faradaic effeciency enhancement with the addition of Br⁻ to TEMPO, compared to TEMPO only, which has a Faradaic efficiency of 33.7%. As a note, the exact oxidized Br⁻ species that interacts with TEMPO has not yet been identified, hence referring to the oxdized Br⁻ species as OBS. Lastly, the current system is not specific towards the generation of a single oxidized EtOH species, given that the Faradaic efficiency of 59.5% for the Br⁻ and TEMPO system pertains to 9.7% towards acetaldehyde, 37.5% towards acetic acid, and 12.3% towards acetal; therefore, future research should focus on adjusting the Br⁻ and TEMPO system to optimize the Faradaic effeciency towards a specific EtOH oxidized species.

Conclusion

Through this research, progress has been made towards creating renewable means to generate oxidized ethanol and HMF products, through studying $PhCH_2OH$ oxidation. So far, research regarding NO_3^- mediated oxidation of $PhCH_2OH$ in MeCN is an avenue with concerns that question the value of the system. Unfortunately, it was found that NO_3^- requires a base, such as 2,6-lutidine, to be catalytic, and reactions between $NO_3\bullet$ and MeCN indicate that organic solvents may not be suitable for NO_3^- mediated systems. As a result, research on Cl^- and Br^- assisted alcohol oxidation in aqueous conditions was pursued. Though Cl^- has not demonstrated any enhancement in assisting the oxidation of $PhCH_2OH$, Br^- appears to assist in ethanol oxidation. The results pertaining to the combination of Br^- and TEMPO in assisting ethanol oxidation appear promising, though the system currently fails to have specificity regarding the product generated from ethanol oxidation. Therefore, future research will focus on fine tuning the system to achieve a specific product.

<u>Acknowledgements</u>

Resources

1. DiMeglio, J. L.; Terry, B. D.; Breuhaus-Alvarez, A. G.; Whalen, M. J. Base-Assisted Nitrate Mediation as the Mechanism of Electrochemical Benzyl Alcohol Oxidation. *Submitted Manuscript*.

2. Tuck, C. O.; Perez, E.; Horvath, I. T.; Sheldon, R. A.; Poliakoff, M. Valorization of Biomass: Deriving More Value from Waste. *Science* **2012**, *337* (6095), 695–699. https://doi.org/10.1126/science.1218930.

3. Antal, M. J.; Mok, W. S. L.; Richards, G. N. Mechanism of Formation of 5-(Hydroxymethyl)-2-Furaldehyde from d-Fructose and Sucrose. *Carbohydrate Research* **1990**, *199* (1), 91–109. https://doi.org/10.1016/0008-6215(90)84096-D.

4. Priecel, P.; Endot, N. A.; Carà, P. D.; Lopez-Sanchez, J. A. Fast Catalytic Hydrogenation of 2,5-Hydroxymethylfurfural to 2,5-Dimethylfuran with Ruthenium on Carbon Nanotubes. *Ind. Eng. Chem. Res.* **2018**, *57* (6), 1991–2002. https://doi.org/10.1021/acs.iecr.7b04715.

5. Chatterjee, M.; Ishizaka, T.; Kawanami, H. Hydrogenation of 5-Hydroxymethylfurfural in Supercritical Carbon Dioxide–Water: A Tunable Approach to Dimethylfuran Selectivity. *Green Chem.* **2014**, *16* (3), 1543. https://doi.org/10.1039/c3gc42145g.

6. Huang, Y.-B.; Chen, M.-Y.; Yan, L.; Guo, Q.-X.; Fu, Y. Nickel-Tungsten Carbide Catalysts for the Production of 2,5-Dimethylfuran from Biomass-Derived Molecules. *ChemSusChem* **2014**, *7* (4), 1068–1072. https://doi.org/10.1002/cssc.201301356.

7. Mabbott, G. A. An Introduction to Cyclic Voltammetry. *J. Chem. Educ.* **1983**, *60* (9), 697. https://doi.org/10.1021/ed060p697.

8. Pietrzyk, D. J.; Frank, C. W. Introduction to Electrochemistry. In *Analytical Chemistry*; Elsevier, 1979; pp 581–597. https://doi.org/10.1016/B978-0-12-555160-1.50032-0.

9. Bard, A. J.; Faulkner, L. R. *Electrochemical Methods: Fundamentals and Applications*, 2nd ed.; Wiley: New York, 2001.

10. Leonard, J. E.; Scholl, P. C.; Steckel, T. P.; Lentsch, S. E.; Van De Mark, M. R. Electrochemical Oxidation of Alcohols: Part II Preparative Anodic Oxidation of Secondary Alkanols Employing Lithium Nitrate. *Tetrahedron Letters* **1980**, *21* (49), 4695–4698. https://doi.org/10.1016/0040-4039(80)88096-8.

11. DiMeglio, J. L.; Breuhaus-Alvarez, A. G.; Li, S.; Bartlett, B. M. Nitrate-Mediated Alcohol Oxidation on Cadmium Sulfide Photocatalysts. *ACS Catal.* **2019**, *9* (6), 5732–5741. https://doi.org/10.1021/acscatal.9b01051.

12. Terry, B. D.; DiMeglio, J. L.; Cousineau, J. P.; Bartlett, B. M. Nitrate Radical Facilitates Indirect Benzyl Alcohol Oxidation on Bismuth(III) Vanadate

Photoelectrodes. *ChemElectroChem* **2020**, *7* (18), 3776–3782. https://doi.org/10.1002/celc.202000911.

13. Reddy, S. R.; Stella, S.; Chadha, A. Simplified Procedure for TEMPO-Catalyzed Oxidation: Selective Oxidation of Alcohols, α -Hydroxy Esters, and Amides Using TEMPO and Calcium Hypochlorite. *Synthetic Communications* **2012**, *42* (23), 3493–3503. https://doi.org/10.1080/00397911.2011.584650.

14. Okada, T.; Asawa, T.; Sugiyama, Y.; Iwai, T.; Kirihara, M.; Kimura, Y. ChemInform Abstract: Sodium Hypochlorite Pentahydrate (NaOCl·5H$_2$O) Crystals; An Effective Re-Oxidant for TEMPO Oxidation. *ChemInform* **2016**, *47* (38). https://doi.org/10.1002/chin.201638041.

15. Anelli, P. T.; Biffi, C.; Montanari, F.; Quici, S. Fast and Selective Oxidation of Primary Alcohols to Aldehydes or to Carboxylic Acids and of Secondary Alcohols to Ketones Mediated by Oxoammonium Salts under Two-Phase Conditions. *J. Org. Chem.* **1987**, *52* (12), 2559-2562. https://doi.org/10.1021/jo00388a038.